

pubs.acs.org/macroletters Letter

Norbornene Dicarboximide: A Green Alternative for Thiol-Norbornene Photopolymers

Warrick Ma, Nathaniel Wright, and Yadong Wang*



Cite This: *ACS Macro Lett.* 2024, 13, 915–920



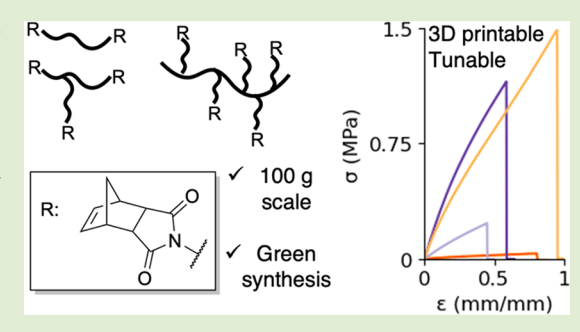
ACCESS I

Metrics & More

Article Recommendations

s Supporting Information

ABSTRACT: Carbic anhydride is an underappreciated starting material for 3D-printable, non-hydrogel photopolymers. Compared with other norbornene precursors, carbic anhydride is cheaper and reactive via aminolysis. As a result, the generalized and efficient functionalization with carbic anhydride can increase the utilization of thiol-norbornene photopolymers. Here, we report carbic anhydride's catalyst-free condensation with two commodity polymers: amine-functionalized polypropylene glycol and polydimethylsiloxane. The reaction completes in 1 h, produces water as the only byproduct, and does not require purification. It is therefore affordable, facile, and green. Mixing the product with thiol cross-linkers and the appropriate photoadditives produces photopolymers that are printable via Digital Light



Processing. The photopolymers exhibit tunable tensile properties and a functional surface by varying the polymer backbone and thiol stoichiometry. Moreover, the photopolymers are 3D-printed into true-to-scale human aorta models and porous scaffolds with high resolution. The simple yet versatile platform will benefit additive manufacturing of soft materials and beyond.

hiol-norbornene photopolymers are excellent for vat photopolymerization due to their facile click chemistry. 1,2 Nevertheless, their 3D-printing is mainly limited to hydrogels that comprise norbornene-functionalized gelatin, hyaluronic acid, methylcellulose, and chitosan.^{2,3} An exception is 4Degra, a 3D-printable photopolymer that comprises polycarbonate with pendant norbornenes. In addition, we recently reported a 3D-printable triblock copolyester comprising norbornene repeating units. Nevertheless, thiol-norbornene photopolymers are difficult to scale because their synthesis uses toxic coupling agents, laborious purification, and, in some cases, moisture-sensitive catalysts. While thiol cross-linkers are commodity chemicals, a common norbornene-functionalized macromer—such as norbornene-functionalized polyethylene glycol—costs \$315 for 1 g.6 This is more expensive than a 12K resolution Digital Light Processing (DLP) printer (ANY-CUBIC Photon Mono M5s, \$269). Because most DLP printers need at least 30 mL of photopolymer to coat the bottom of the resin vat, available norbornene-functionalized macromers are too cost-prohibitive to 3D print at scale.

Thus, scalable thiol-norbornene photopolymers need a more affordable starting material and a more scalable synthesis. Among the norbornene precursors, carbic anhydride (CA) is the cheapest and greenest. For example, CA is produced via a Diels—Alder reaction of cyclopentadiene with maleic anhydride: the latter can be derived from sustainable feedstocks and hydrolyzed to maleic acid, a natural metabolite. This sharply contrasts 5-norbornene-2-carboxylic acid, which uses acrylic acid—a nonsustainable and carcinogenic feedstock—as the dienophile. On the other hand, CA reacts via alcoholysis or

aminolysis, thermodynamically favorable processes that can take place without a catalyst. If water is removed from the reaction mixture, CA's reaction with amine yields norbornene dicarboximide. Adapting this strategy—yet to be explored in vat photopolymerization—will make the synthesis of thiolnorbornene photopolymers greener and more economical.

The norbornene dicarboximide-functionalized polymers are synthesized from amine-functionalized PPG and PDMS (Scheme 1). Toluene removes the water azeotropically and affords a homogeneous reaction mixture. Regardless of the molecular weight or the amine's steric hindrance, all reactions proceed to ~100% conversion within 1 h, as verified by water collected in a Dean-Stark trap. ¹H NMR indicates the clean formation of norbornene dicarboximide from the singlet at 6.0-6.1 ppm (Figure 1). Except for 7kPDMS-5CA, all products are transparent liquids. 7kPDMS-5CA's opacity potentially arises from the partial crystallinity of the pendant norbornene dicarboximide propyl side chains. Overall, this green, catalyst-free, and efficient synthesis uses recyclable toluene, produces water, and does not require any purification, thus reducing the cost and difficulty of norbornene functionalization.

Received: May 19, 2024 Revised: July 3, 2024 Accepted: July 9, 2024 Published: July 11, 2024





Scheme 1. Synthesis of Norbornene Dicarboximide Polymers from Amine-Functionalized Polypropylene Glycol (PPG) or Polydimethylsiloxane (PDMS)^a

$$H_2N$$
 O_n NH_2 $M_nPPG-2CA$ $M_nPDMS-2CA$ $M_nPDMS-2CA$ $M_nPDMS-2CA$ $M_nPDMS-2CA$ $M_nPPG-3CA$ M_nPP

^aThe prefix M_n represents the average molecular weight of the amine-functionalized starting material. The number preceding CA represents the number of norbornene dicarboximide groups in a single chain. For example, amine-terminated PPG ($M_n = 2 \text{ kDa}$) affords 2kPPG-2CA.

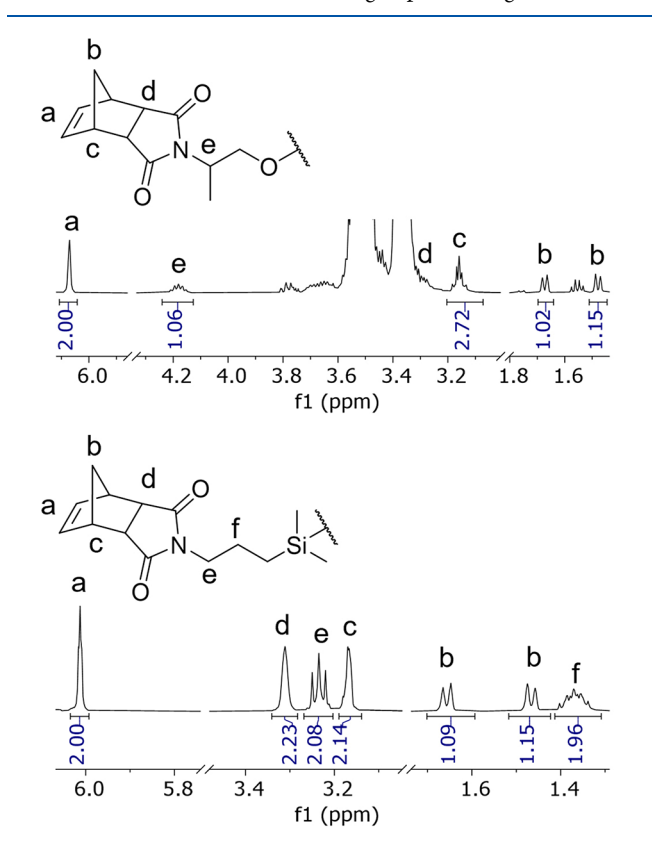


Figure 1. ¹H NMR spectra of norbornene dicarboximide-functionalized polymers showing their end group structure (500 MHz, CDCl₃). Full spectra are in the Supporting Information (Figures S1 and S2).

Two thiol cross-linkers, pentaerythritol tetrakis(3-mercapto-propionate) (PETMP) and 4–6% (mercaptopropyl)-methylsiloxane]-dimethylsiloxane copolymer (polySH), are used to study photopolymerization. PETMP is miscible with PPG-based polymers but not with PDMS-based polymers. As a result, 0.9kPDMS-2CA:PETMP is a milky-white mixture. We

attempted to solubilize PDMS-based polymers with polySH, which has an M_n of 6-8 kDa and five mercaptopropyl groups per chain on average. However, only 5kPDMS-2CA:polySH is transparent. All immiscible mixtures remain stable emulsions after overnight storage without agitation. 0.9kPDMS-2CA:polySH forms stable, micellar aggregates via an unfavorable interaction between the nonpolar PDMS backbone and the polar PETMP. The relatively polar norbornene dicarboxamide is probably at the exterior to react with PETMP. The immiscibility of 7kPDMS-5CA:polySH is more challenging to explain because 7kPDMS-5CA begins as a milky-white liquid. Favorable interactions between norbornene dicarboximide and mercaptopropyl side chains should still occur. Regardless, aggregate formation may lead to a heterogeneous network and affect the mechanical properties of 3D-printed materials. 10 However, further investigation is outside the scope of this report, and the homogenization of PDMS in aliphatic polymers to improve their mechanical properties is still under active research.

To assess the printability of norbornene dicarboximide photopolymers, we investigated their photorheology with 400-500 nm light to capture the common 405 nm wavelength used in many resin printers. Judging by the crossover point of loss modulus and storage modulus, only 5kPPG-3CA:PETMP cross-links too slowly (Figure S3) for DLP printing (385 or 405 nm). Cross-linked 5kPPG-3CA:PETMP is also extremely soft and tacky, indicative of a weak network not suitable for DLP 3D-printing. We initially suspected the partial norbornene functionalization would lead to inefficient cross-linking. However, diffusion NMR of 5kPPG-3CA confirms all norbornenes are covalently linked to the PPG backbone (Figure S4). Therefore, 5kPPG-3CA:PETMP's weak mechanical properties may arise from its imperfect network structures (i.e., macrocycles that do not increase the cross-linking density). All other photopolymers cross-link quickly, with various crossover points (Figure 2, Figure S3) reflecting the structure-property relationships. 7kPDMS-5CA:polySH crosslinks much faster than 5kPDMS-2CA:polySH because the

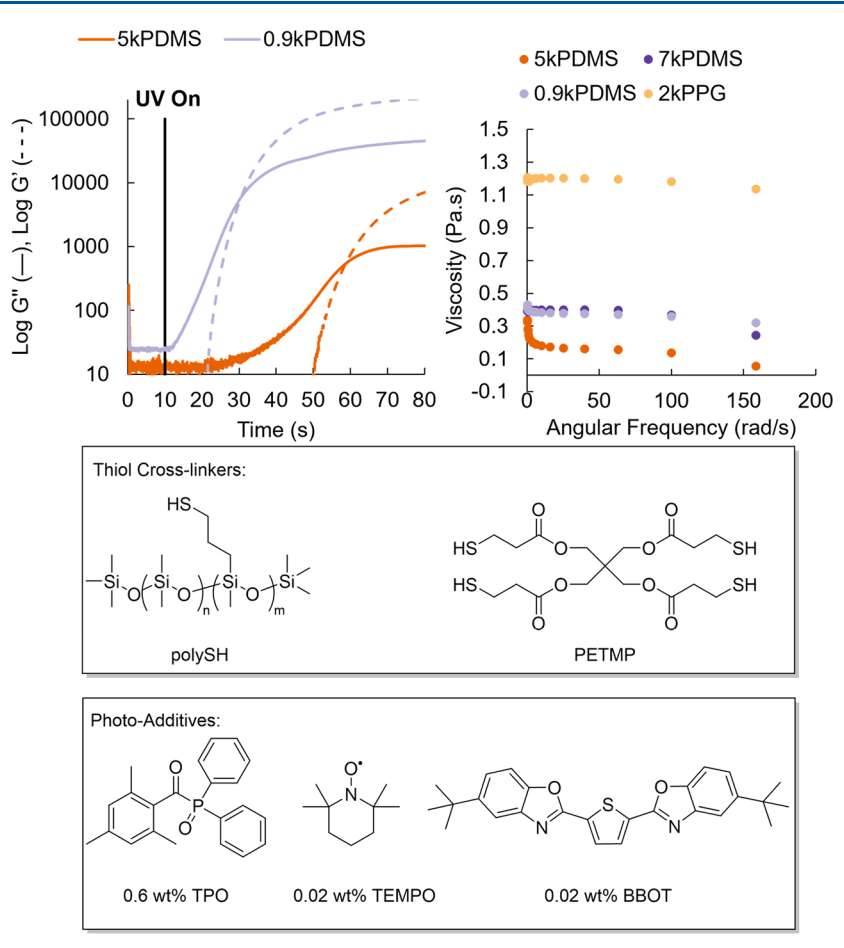


Figure 2. Photorheology and viscosity of representative photopolymers (names are abbreviated to their respective backbone; see Table 1 for details). The photorheology data of 2kPPG and 7kPDMS are in Figure S3. Ultraviolet (UV) radiation (400-500 nm, 10 mW/cm²) is switched on at 10 s (G', storage modulus; G'', loss modulus). The cross-linker is either polySH or PETMP, and all formulations use the same photoadditives. Diphenyl (2,4,6-trimethylbenzoyl)-phosphine oxide (TPO) initiates UV cross-linking; 2,2,6,6-tetramethylpiperidine 1-oxyl (TEMPO) scavenges radicals to increase resin shelf life and resolution; and 2,5-bis(5-tert-butyl-2-benzoxazolyl)thiophene (BBOT) absorbs UV to reduce UV penetration depth.

Table 1. Properties of Various Photopolymers

Photopolymer ^a	$E (MPa)^c$	$arepsilon_{ ext{max}}^{c}$	$\sigma_{ m max}~({ m MPa})^c$	$T_{g} (^{\circ}C)^{d}$
2kPPG-2CA:PETMP	3.0 ± 0.1	$57\% \pm 4\%$	1.1 ± 0.1	-49
0.9kPDMS-2CA:PETMP ^b	2.1 ± 0.1	$97\% \pm 2\%$	1.5 ± 0.1	-8
7kPDMS-5CA:polySH	0.6 ± 0.07	$45\% \pm 1\%$	0.2 ± 0.07	N/A ^e
5kPDMS-2CA:polySH ^b	0.08 ± 0.006	$82\% \pm 1\%$	0.03 ± 0.001	N/A^e

^aAll photopolymers are 3D printable. ^bOpaque photopolymers with a milky-white color. ^cDerived from uniaxial tensile testing (n = 3). E, Young's modulus; E_{max} strain-at-failure; σ_{max} ultimate tensile strength. ^dMeasured via differential scanning calorimetry (DSC) on the second heating ramp. ^eNot detected in the DSC temperature range (-80 to 120 °C).

former has a higher norbornene concentration. Given these results, the heterogeneity of 0.9kPDMS-2CA:PETMP, 7kPDMS-5CA:polySH, and 5kPDMS-2CA:polySH does not jeopardize the photo-cross-linking. Lastly, the complex viscosity of all formulations is well below 5 Pa·s (Figure 2), which is the upper viscosity limit of commercial DLP printers. LkPPG-2CA:PETMP is the most viscous due to PPG's higher crystallinity than PDMS. Among the PDMS-based photopolymers, 7kPDMS-5CA:polySH is the most viscous due to its PDMS backbone having a higher molecular weight.

After rheological studies identified four printable formulations (Table 1), we 3D-printed dog-bone-shaped specimens to study their mechanical properties (Figure 3A, Table 1), as well

as two challenging structures, true-to-scale human aorta and porous scaffolds (Figure 3B-D), to showcase their printability on a commercial DLP printer. Of note, the photopolymers composed of PDMS(7kPDMS-5CA:polySH and 5kPDMS-2CA:polySH) do not display $T_{\rm g}$ in the DSC temperature range ($-80-120~{\rm ^{\circ}C}$). This result agrees with the extremely low $T_{\rm g}$, $-120~{\rm ^{\circ}C}$, of commercial PDMS elastomers. Switching the thiol cross-linker to PETMP increases the $T_{\rm g}$ to $-8~{\rm ^{\circ}C}$, as observed for 0.9kPDMS-2CA:PETMP (Table 1). The higher $T_{\rm g}$ reflects a higher cross-linking density, which is the result of PETMP having a lower molecular weight and a shorter PDMS backbone. Compared with 0.9kPDMS-2CA:PETMP, 2kPPG-2CA:PETMP has a much lower $T_{\rm g}$ ($-49~{\rm ^{\circ}C}$, Table 1) because of its longer backbone and lower cross-linking density. Low $T_{\rm g}$

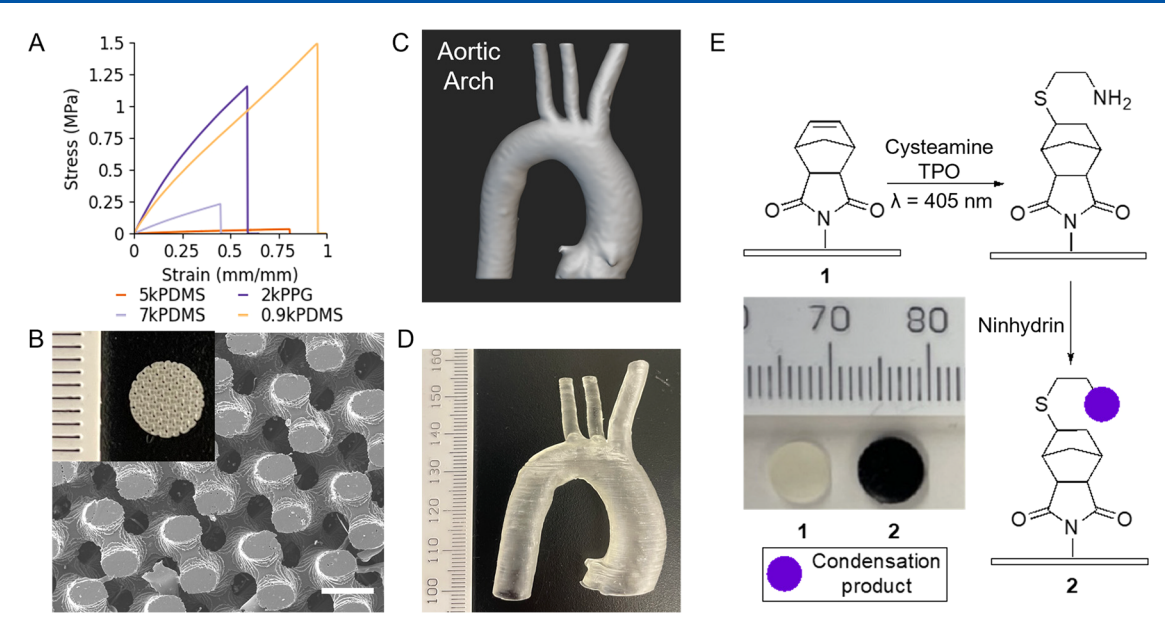


Figure 3. (A) Representative stress—strain curves of 3D printed thiol-norbornene networks (photopolymers' names are abbreviated to their polymer backbone due to space constraints). (B) Photograph and scanning electron microscopy (SEM) image (scale bar: $500 \mu m$) of a porous gyroid puck and a porous gyroid puck tube; pores are estimated to be $200-300 \mu m$ in diameter. (C, D) High-fidelity DLP 3D-printing of a true-to-scale aortic arch rendered from patient Computed Tomography (CT) scans. (E) Surface functionalization with cysteamine. The ruler division is 1 mm.

ensures soft elasticity at room temperature. The absence of melting and crystallization corresponds with the thermal properties of the PPG and PDMS backbones and reflects the limited chain mobility of cross-linked networks.

Next, we investigated the effect of the average molecular weight between each cross-linking point (M_c) on the tensile properties. The 1:1 reactivity of thiol-norbornene generates evenly spaced cross-links.^{1,2} Therefore, for 2kPPG-2CA:-PETMP and 0.9kPDMS-2CA:PETMP, M_n of their polymer precursors approximates the M_c . For 7kPDMS-5CA:polySH and 5kPDMS-2CA:polySH, M_c is inferred by the assumed even distribution of mercaptopropyl groups along the polySH backbone. Uniaxial tensile testing reveals a general trend among the PDMS-based photopolymers: Young's modulus and ultimate tensile strength inversely correlate with the M_c (Table 1, Figure 3A). The low molecular weight of PETMP, its tetra functionality, and the 0.9-kDa PDMS backbone culminate in the high Young's modulus ($E = 2.1 \pm 0.1$ MPa) and high tensile strength (σ_{max} = 1.5 \pm 0.1 MPa) of 0.9kPDMS-2CA:PETMP. Switching the backbone to PPG ($M_n = 2 \text{ kDa}$) yields a stiffer network despite a higher M_c , as observed for 2kPPG-2CA:PETMP (Table 1, $E = 3.0 \pm 0.1$ MPa). PPG's high crystallinity might have contributed to its improved stiffness.

To demonstrate the printability of our system, we first printed porous gyroid pucks (Figure 3B) and a porous gyroid tubular scaffold (Figure S5) with 2kPPG-2CA:PETMP and 0.9kPDMS-2CA:PETMP. Scanning electron microscopy (SEM) shows well-resolved pore structures (Figure 3B, Figure S5), matching the overall shape of the STL model. We then printed true-to-scale human aortas with the two softest elastomers,5kPDMS-2CA:polySH and 7kPDMS-5CA:polySH. We selected the aorta model for two reasons. First, it is important in medical education, surgical planning, etc. In addition, the hollow structure has thin walls (<1 mm) and overhangs; features that are challenging to achieve with 3D-

printing. 7kPDMS-5CA:PETMP withstands the suction force generated by the hollow structure upon elevation from the bottom of the resin vat. The well-resolved local features, arch, and arterial branches indicate excellent printability (Figure 3C,D, Figure S6). 0.9kPDMS-2CA:PETMP and 2kPPG-2CA:PETMP, however, adhere more to the fluorinated ethylene propylene (FEP) film of the resin vat and cannot print the thin-walled model. Increasing the wall thickness to 2 mm solves this problem by reinforcing the model (Figure S7). For 5kPDMS-2CA which has the lowest Young's modulus ($E = 0.08 \pm 0.006$ MPa), a 2 mm wall is necessary to stabilize the ultrasoft model during printing.

Compared with acrylate photopolymers, the off-stoichiometric effect is a major advantage of the thiol-norbornene system. The thiol cross-linker as the limiting reagent results in a softer network and a functional surface furnishing unreacted norbornenes. Using 0.9kPDMS-2CA as the model, we added 0.7 eq of PETMP to form the off-stoichiometric photopolymer, which remains printable but has lower tensile properties (E = 0.36 ± 0.04 MPa, $\varepsilon_{\rm max}$ = 66% \pm 2%, $\sigma_{\rm max}$ = 0.20 \pm 0.02 MPa). A lower glass transition temperature ($T_g = -37$ °C) confirms the lower cross-linking density. Detecting unreacted norbornenes using Fourier-Transform Infrared Spectroscopy (FT-IR) fails, as the C=C stretch of norbornene is eclipsed by the carbonyl C=O stretch of PETMP (Figure S8). Therefore, we converted unreacted norbornenes to amines by grafting cysteamine via thiol-norbornene click chemistry. 3D-printed pucks were exposed to a methanolic cysteamine solution containing 1 wt % TPO at room temperature with or without UV light for 1 h. After thoroughly washing the pucks with ethanol, we placed them in a ninhydrin solution. The sensitive ninhydrin assay detects the resultant free amines by forming a purple imine product colloquially known as Ruhemann's purple. 13 As thiol-norbornene click chemistry cannot proceed via base catalysis or without radicals, pucks without UV exposure serve as negative controls. Pucks exposed to UV start

turning purple within 30 s and become dark purple within a few minutes. Negative controls do not display color changes in the same time frame. This drastic difference proves the feasibility of surface modification of off-stoichiometric thiol—ene photopolymers.¹⁴

Next, we compared norbornene dicarboximide photopolymers with literature precedents. To our knowledge, PPG-based thiol—ene photopolymers have never been reported before. As expected, PPG diacrylate ($M_{\rm n}=0.4-2~{\rm kDa}$) cross-links into stiff ($E=263-3366~{\rm MPa}$), brittle ($\varepsilon_{\rm max}=2-12\%$) materials that require 5–30 vol % PPG ($M_{\rm n}=0.4~{\rm kDa}$) diluent to be printable via DLP. ¹⁵ 2kPPG-2CA:PETMP is therefore more advantageous for soft elastomer applications. The mechanical properties of photopolymers based on 2kPPG-2CA can be further tuned via thiol stoichiometry and the length of the PPG backbone.

In contrast, PDMS-based thiol—ene photopolymers have applications in soft robotics and microfluidics. ¹⁶ The appeal lies in 3D-printing's efficiency and versatility, which soft lithography hardly possesses. ^{17–19} Vinyl- and methacrylate-functionalized PDMS are commercially available and mixing them with thiol cross-linkers like polySH affords 3D-printable photopolymers. However, norbornene functionalization is more advantageous due to its green synthesis presented thus far and documented use in biorthogonal click chemistry. As a result, we examined whether norbornene dicarboxamide-functionalized PDMS exhibits the same mechanical performance.

Wallin et al. used a blend of bifunctional vinyl-terminated PDMS and polySH ($M_p = 4-6$ kDa, 2.5% or 5% thiol) to 3Dprint soft robots that self-heal via thiol-ene click reactions from pockets of unreacted resins. 16 Vinyl-terminated PDMS $(M_n = 6 \text{ kDa})$ cross-linked with polySH $(M_n = 4-6 \text{ kDa}, 5\%)$ thiol) has a Young's modulus of 0.09 kPa and a strain-at-failure of 76%. 5kPDMS-2CA:polySH has similar tensile properties. This agreement is not surprising, because 5kPDMS-2CA:polySH has similar molecular weights and alkene and thiol functionalities. Fleck et al. reported a printable photopolymer comprising a methacrylate-PDMS copolymer and polySH (E = 11.5 MPa, $\varepsilon_{\rm max}$ = 12%). The higher degree of methacrylate and thiol functionalities (7-9%), as well as the potential free radical cross-linking of methacrylate, contribute to the high stiffness and low strain-at-failure. Additionally, the high viscosity (~4 Pa·s) may jeopardize resolution. In their follow-up work, replacing multifunctional methacrylate-PDMS with methacryloxypropyl-terminated PDMS not only reduced the resin viscosity to ~0.5 Pa·s, but lowered the Young's modulus to 0.3 MPa and increased the strain-at-failure to 59%. 19 Compared with these precedents, norbornene dicarboximide-functionalized PDMS performs similarly. Although adding functionality such as thiourea can further improve mechanical properties, ²⁰ it is beyond the scope of this preliminary report.

In conclusion, the catalyst-free condensation between amine-functionalized PPG or PDMS and CA affords a family of norbornene dicarboximide functionalized polymers—with water as the only byproduct. The reaction is affordable and green and occurs at a 100-g scale without purification. The product constitutes a novel platform for thiol-norbornene photopolymers—which have tunable Young's modulus, excellent printability on a commercial DLP printer, and a surface for click chemistry modification. Because the molecular weight of amine starting materials ranges from 0.8 to 7 kDa, we

expect our method to be compatible with commodity small-molecule amines and other high-molecular-weight, amine-functionalized polymers. The broad substrate scope affords a highly rigid or ultrasoft thiol-norbornene network, or anywhere in between. Cheap but versatile, our method can benefit additive manufacturing of soft materials and beyond.

ASSOCIATED CONTENT

Supporting Information

The Supporting Information is available free of charge at https://pubs.acs.org/doi/10.1021/acsmacrolett.4c00334.

Materials and Methods, ¹H NMR spectra, photorheology data, and FT-IR spectra (PDF)

AUTHOR INFORMATION

Corresponding Author

Yadong Wang — Meinig School of Biomedical Engineering, College of Engineering, Cornell University, Ithaca, New York 14853-1801, United States; orcid.org/0000-0003-2067-382X; Email: yw839@cornell.edu

Authors

Warrick Ma – Department of Chemistry and Chemical Biology, Baker Laboratory, Cornell University, Ithaca, New York 14853-1801, United States; occid.org/0000-0003-3622-4981

Nathaniel Wright — Meinig School of Biomedical Engineering, College of Engineering, Cornell University, Ithaca, New York 14853-1801, United States

Complete contact information is available at: https://pubs.acs.org/10.1021/acsmacrolett.4c00334

Author Contributions

The manuscript was written through contributions of all authors. All authors have given approval to the final version of the manuscript. CRediT: Warrick Ma conceptualization, data curation, formal analysis, investigation, methodology, project administration, resources, software, validation, visualization, writing-original draft; Nathaniel Wright data curation, methodology, resources, validation, writing-review & editing; Yadong Wang funding acquisition, supervision, writing-review & editing.

Notes

The authors declare no competing financial interest. STL files are deposited in https://github.com/warrickma/STL model.

ACKNOWLEDGMENTS

The authors thank Jonathan W. Weinsaft, M.D., for providing the anonymized patient CT data and Dr. Anthony R. D'Amato for generating the artery STL model. This work made use of the CCMR Shared Experimental Facilities and the NMR Facility at Cornell University, which are supported by the NSF (DMR-1719875 and CHE-1531632, respectively). This work was supported by an Ignite Innovation Acceleration Grant from the Center for Technology Licensing, Cornell University.

REFERENCES

(1) Bagheri, A.; Jin, J. Photopolymerization in 3D Printing. ACS Applied Polymer Materials 2019, 1 (4), 593–611. Yeazel-Klein, T. R.; Davis, A. G.; Becker, M. L. Thiol-ene-Based 3D Printing of Bioresorbable Fumarate-Based ABA Triblock Copolyester Elastomers.

- Adv. Mater. Technol. 2023, 2201904. Kirillova, A.; Yeazel, T. R.; Gall, K.; Becker, M. L. Thiol-Based Three-Dimensional Printing of Fully Degradable Poly(propylene fumarate) Star Polymers. ACS Appl. Mater. Interfaces 2022, 14 (34), 38436–38447. Ooi, H. W.; Mota, C.; ten Cate, A. T.; Calore, A.; Moroni, L.; Baker, M. B. Thiol-Ene Alginate Hydrogels as Versatile Bioinks for Bioprinting. Biomacromolecules 2018, 19 (8), 3390–3400. Oesterreicher, A.; Gorsche, C.; Ayalur-Karunakaran, S.; Moser, A.; Edler, M.; Pinter, G.; Schlogl, S.; Liska, R.; Griesser, T. Exploring Network Formation of Tough and Biocompatible Thiol-yne Based Photopolymers. Macromol Rapid Comm 2016, 37 (20), 1701–1706. Sticker, D.; Rothbauer, M.; Lechner, S.; Hehenberger, M. T.; Ertl, P. Multilayered, membrane-integrated microfluidics based on replica molding of a thiol-ene epoxy thermoset for organ-on-a-chip applications. Lab Chip 2015, 15 (24), 4542–4554.
- (2) Göckler, T.; Haase, S.; Kempter, X.; Pfister, R.; Maciel, B. R.; Grimm, A.; Molitor, T.; Willenbacher, N.; Schepers, U. Tuning Superfast Curing Thiol-Norbornene-Functionalized Gelatin Hydrogels for 3D Bioprinting. *Adv. Healthc Mater.* **2021**, *10* (14), 2100206. Zhu, Y. Z.; Shen, J.; Yin, L.; Wei, X. J.; Chen, F.; Zhong, M. Q.; Gu, Z.; Xie, Y.; Jin, W.; Liu, Z.; et al. Directly photopatterning of polycaprolactone-derived photocured resin by UV-initiated thiol-ene "click" reaction: Enhanced mechanical property and excellent biocompatibility. *Chem. Eng. J.* **2019**, *366*, 112–122.
- (3) Galarraga, J. H.; Dhand, A. P.; Enzmann, B. P.; Burdick, J. A. Synthesis, Characterization, and Digital Light Processing of a Hydrolytically Degradable Hyaluronic Acid Hydrogel. *Biomacromolecules* **2023**, 24 (1), 413–425.
- (4) Weems, A. C.; Arno, M. C.; Yu, W.; Huckstepp, R. T. R.; Dove, A. P. 4D polycarbonates via stereolithography as scaffolds for soft tissue repair. *Nat. Commun.* **2021**, *12* (1), 3771.
- (5) Ma, W. R.; Miller, P. G.; Wang, Y. D. ABA Block Copolyester Thiol-Ene Resin From Triethylborane-Assisted Ring-Opening Copolymerization. ACS Applied Polymer Materials 2024, 6 (2), 1503–1513.
- (6) Creative PEGWorks. Norbornene-PEG-Norbornene, MW 2k. https://creativepegworks.com/product/norbornene-peg-norbornene-mw-2k-5g (accessed June 25, 2024).
- (7) ANYCUBIC. Anycubic Photon Mono M5s. https://store.anycubic.com/products/photon-mono-m5s (accessed June 25, 2024).
- (8) Cucciniello, R.; Cespi, D.; Riccardi, M.; Neri, E.; Passarini, F.; Pulselli, F. M. Maleic anhydride from bio-based 1-butanol and furfural: a life cycle assessment at the pilot scale. *Green Chem.* **2023**, 25 (15), 5922–5935.
- (9) Wang, H.; Ma, C. H.; Han, Z. Y.; Liao, X. J.; Sun, R. Y.; Xie, M. R. Efficient synthesis of trefoil-shaped tricyclic polymers by a ROMP-based blocking-cyclization technique. *Polym. Chem-Uk* **2024**, *15* (6), 534–543. Majchrzak, M.; Hine, P. J.; Khosravi, E. An autonomous self-healing system based on ROMP of norbornene dicarboximide monomers. *Polymer* **2012**, *53* (23), 5251–5257. Pawloski, A. R.; Nealey, P. F.; Conley, W. Efficiency of photoacid generators in chemically amplified resists for 157nm lithography. *J. Photopolym. Sci. Technol.* **2002**, *15* (5), 731–739.
- (10) Abdilla, A.; D'Ambra, C. A.; Geng, Z. S.; Shin, J. J.; Czuczola, M.; Goldfeld, D. J.; Biswas, S.; Mecca, J. M.; Swier, S.; Bekemeier, T. D.; et al. Silicone-based polymer blends: Enhancing properties through compatibilization. *J. Polym. Sci.* **2021**, *59* (19), 2114–2128.
- (11) Wu, Y. L.; D'Amato, A. R.; Yan, A. M.; Wang, R. Q.; Ding, X. C.; Wang, Y. D. Three-Dimensional Printing of Poly(glycerol sebacate) Acrylate Scaffolds via Digital Light Processing. ACS Appl. Bio Mater. 2020, 3 (11), 7575–7588.
- (12) Brounstein, Z.; Zhao, J. C.; Geller, D.; Gupta, N.; Labouriau, A. Long-Term Thermal Aging of Modified Sylgard 184 Formulations. *Polymers-Basel* **2021**, *13* (18), 3125.
- (13) Kaiser, E.; Colescott, R. L.; Bossinger, C. D.; Cook, P. I. Color test for detection of free terminal amino groups in the solid-phase synthesis of peptides. *Anal. Biochem.* **1970**, 34 (2), 595–598.
- (14) Stanfield, M. K.; Kotlarewski, N.; Smith, J.; Thickett, S. C. Biobased Transparent Thiol-Ene Polymer Networks from Levoglu-

- cosan. ACS Applied Polymer Materials 2024, 6 (1), 837–845. Shahzadi, L.; Maya, F.; Breadmore, M. C.; Thickett, S. C. Functional Materials for DLP-SLA 3D Printing Using Thiol-Acrylate Chemistry: Resin Design and Postprint Applications. ACS Applied Polymer Materials 2022, 4 (5), 3896–3907.
- (15) Pongwisuthiruchte, A.; Dubas, S. T.; Aumnate, C.; Potiyaraj, P. Mechanically tunable resins based on acrylate-based resin for digital light processing (DLP) 3D printing. *Sci. Rep.* **2022**, *12* (1), 20025.
- (16) Wallin, T. J.; Pikul, J. H.; Bodkhe, S.; Peele, B. N.; Mac Murray, B. C.; Therriault, D.; McEnerney, B. W.; Dillon, R. P.; Giannelis, E. P.; Shepherd, R. F. Click chemistry stereolithography for soft robots that self-heal. *J. Mater. Chem. B* **2017**, *5* (31), 6249–6255.
- (17) Urrios, A.; Parra-Cabrera, C.; Bhattacharjee, N.; Gonzalez-Suarez, A. M.; Rigat-Brugarolas, L. G.; Nallapatti, U.; Samitier, J.; DeForest, C. A.; Posas, F.; Garcia-Cordero, J. L.; et al. 3D-printing of transparent bio-microfluidic devices in PEG-DA. *Lab Chip* **2016**, *16* (12), 2287–2294.
- (18) Fleck, E.; Sunshine, A.; DeNatale, E.; Keck, C.; McCann, A.; Potkay, J. Advancing 3D-Printed Microfluidics: Characterization of a Gas-Permeable, High-Resolution PDMS Resin for Stereolithography. *Micromachines* **2021**, *12*, 1266.
- (19) Fleck, E.; Keck, C.; Ryszka, K.; DeNatale, E.; Potkay, J. Low-Viscosity Polydimethylsiloxane Resin for Facile 3D Printing of Elastomeric Microfluidics. *Micromachines* **2023**, *14*, 773.
- (20) Du, K.; Basuki, J.; Glattauer, V.; Mesnard, C.; Nguyen, A. T.; Alexander, D. L. J.; Hughes, T. C. Digital Light Processing 3D Printing of PDMS-Based Soft and Elastic Materials with Tunable Mechanical Properties. ACS Applied Polymer Materials 2021, 3 (6), 3049–3059.